Expanding Access to High-Resolution Soil pH Measurement: From Smallholder Farms to 200-Hectare Fields

Chase Maxton[1], Eric Lund[1], Tyler Lund[1],
[1]Veris Technologies, Salina, Kansas, USA

A paper from the Proceedings of the
17th International Conference on Precision Agriculture and 11th Brazilian Congress on Precision and Digital Agriculture
13-15 July 2026
Porto Alegre, Brazil

Abstract.

Soil pH is one of the most influential and correctable soil properties affecting crop productivity, yet timely and spatially representative pH measurement remains inconsistent across agricultural systems. Laboratory turnaround time, sampling cost, limited field access, and sub-field variability can all limit the practical resolution of conventional sampling programs.

This study evaluated multiple strategies for delivering actionable soil pH information across diverse production environments. Three deployment approaches using ion-selective electrode technology were assessed: 1) continuous on-the-go soil collection and measurement that generates ~20 pH readings/ha, 2) automated point-based pH providing 2-4 readings/ha 3) and a portable hand-held system suitable for diagnostic testing, specialty or smallholder systems.

To evaluate the relative accuracy of various sensing and sampling densities, a dense soil pH dataset (20 samples/ha) from 18 fields was used as a reference dataset. Lower sampling densities (0.25, 0.40, 1, 2, and 4 ha per sample) were simulated by systematically reducing sampling locations from the reference dataset. Interpolated pH surfaces generated from each density were then compared with the original high-density measurements to quantify accuracy losses associated with reduced sampling intensity. Across the 18 study fields, the greatest pH mapping accuracy was observed at sampling intensities greater than one sample per hectare. Sampling densities of 1 and 2 ha per sample showed diminished accuracy, while the 4 ha density produced greater errors than those associated with a uniform field-average pH estimate. To investigate whether ancillary spatial information could compensate for reduced sampling intensity, a complementary modeling approach was developed using lidar-derived terrain attributes, satellite imagery, and regional soil pH datasets. Across sampling densities from 0.25 to 4 ha per sample, the modeled approach yielded modest improvements in accuracy compared with interpolation of sampled points alone.

Across systems, increasing spatial resolution improved identification of localized acidity and alkalinity constraints that would likely remain undetected under conventional sampling approaches. These findings suggest that scalable, field-based pH measurement strategies can expand access to timely and spatially relevant pH information.

Keywords. Soil pH, acidity, precision, spatial resolution, in situ, modeling, smallholder.

The authors are solely responsible for the content of this paper, which is not a refereed publication. Citation of this work should state that it is from the Proceedings of the 17th International Conference on Precision Agriculture and 11th Brazilian Congress on Precision and Digital Agriculture. EXAMPLE: Last Name, A. B. & Coauthor, C. D. (2026). Title of paper. In Proceedings of the 17th International Conference on Precision Agriculture and 11th Brazilian Congress on Precision and Digital Agriculture (unpaginated, online). Monticello, IL: International Society of Precision Agriculture and Brazilian Congress on Precision and Digital Agriculture.

Introduction

Soil pH affects crop productivity through nutrient availability, toxicity risk, microbial activity, and overall soil function. Because pH is also one of the more correctable soil properties, timely and spatially representative measurement is important for making lime, amendment, and other soil management decisions.

Conventional laboratory sampling remains essential for reliable soil analysis, but practical limits on sampling density can leave important pH variability unresolved. Turnaround time, sampling cost, field access, labor, and the distance between sample points can all limit how precisely acidity or alkalinity patterns are identified. When pH varies within a field at scales smaller than the sampling grid, management zones and variable-rate prescriptions may be based on incomplete spatial information.

Field-based pH sensing offers a practical way to increase measurement density while adapting to different production contexts. Continuous on-the-go systems, automated point-based systems, and portable diagnostic tools each fit different field sizes, crops, equipment access, and decision needs. This study evaluates whether adaptable pH sensing approaches can improve access to timely, spatially relevant pH information while maintaining practical decision value across diverse agricultural systems.

Materials and Methods

Soil pH In-field Measurement Systems

Three methods for collecting soil pH sensor measurements were evaluated. Each method used the same antimony pH electrode but differed in how the sensor engaged the soil. Some systems included additional soil sensors; however, only soil pH measurement performance was evaluated in this study.

Continuous, On-the-go pH

The Veris MSP3 is a tractor-based platform that includes a soil sampling shoe which is automatically controlled to collect soil and then press that sample against antimony pH electrodes on-the-go as the operator traverses the field on typically 15-20 m transects (Fig. 1). A pH measurement is recorded in approximately 10-15 seconds. The electrodes are washed, and the sample shoe moves down to collect a fresh soil sample (Fig. 2). Approximately one pH sensor measurement is taken every 0.05 ha, although exact density depends on operator speed and transect width. The MSP3 also collects soil electrical conductivity (EC) and VisNIR optical data at a 1 Hz rate at the same time.


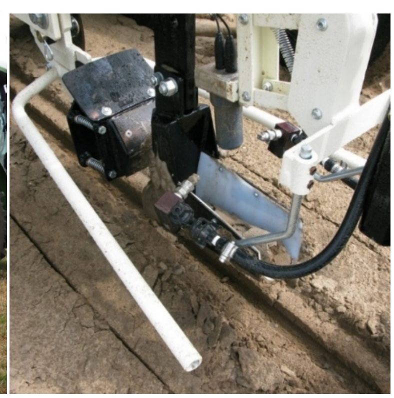

Fig. 1 MSP3 uses tractor hydraulics. Fig. 2 Soil sampling shoe collects the soil

Automated Point-based pH

Two Automated Point-based pH Sensor Platforms were evaluated, the Veris U3 and ProScan. Both systems use electro-hydraulics and can be operated with a UTV or small pickup truck. These platforms automatically measure pH when the pulling vehicle stops at a sampling point. Measurement time is approximately 10 seconds. The density of pH measurements is determined by the transect spacing and operator selection; typical density ranges from a sample every 50 meters to every 65 meters. The U3 model includes EC and VisNIR optical sensing; the optical sensor is built into a metal shoe that opens a 5-8 cm deep furrow in the soil (Fig. 3 and Fig. 4). The pH electrode is then pressed automatically into that furrow.

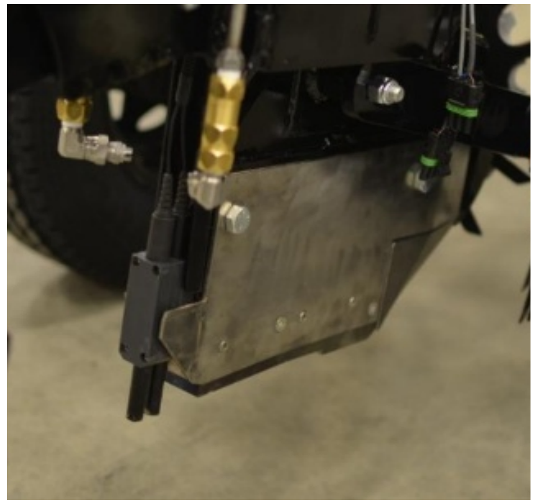

Fig. 3 Veris U3. Fig. 4 U3 pH electrodes use furrow from optical shoe

The ProScan is non-invasive, meaning no part of the platform touches the soil except at the automated sensing location. Since it does not create a furrow, there is a scoop that opens a cavity in the soil for the pH electrode. In addition to pH, the ProScan is equipped with soil EC tines and an ASABE penetrometer tip (ASAE S313.3). Each time the vehicle stops, all 3 sensors collect a reading (Fig. 5 and Fig. 6).

Fig. 5 Veris ProScan

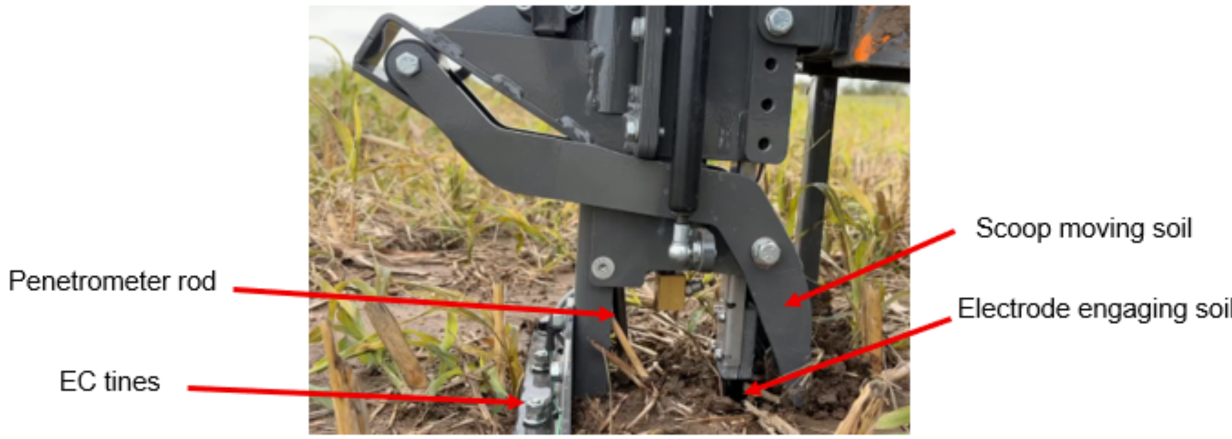

Fig. 6 Soil pH, EC, and penetrometer mechanisms on ProScan

Manual pH

The Scout pH requires the user to place the pH probe in a soil opening at the desired depth (Fig. 7), or into a removed soil core. The user holds antimony electrode in contact with the soil while the measurement is recorded onto a cell phone app (Fig. 8). The user then manually rinses the electrode before inserting into a new sampling location. Total measurement time is approximately 10 seconds. The scouting tool is deployed at a scale relevant to the operator's use case. Crop consultants or growers may target several soil types across larger fields for monitoring lime needs, diagnosing a problem area, or smaller fields could be densely mapped for a precise lime recommendation.

Fig. 7 Scout pH device

Fig. 8 Veris app for iOS and Android smartphone geo-referenced data logging

Map Examples and Accuracy

Below are example maps of the various pH deployments across agriculture fields ranging from 0.8 to 300 ha.

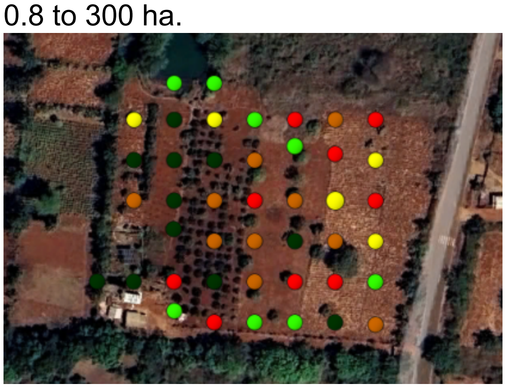

Fig. 9 Manual pH map from 0.8 ha Kenya field

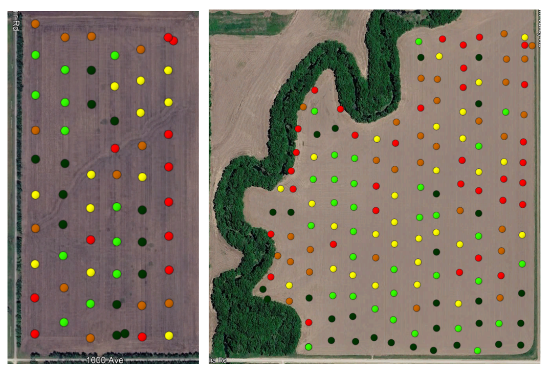

Figures 10 and 11. Automated point-based pH maps from 23 ha and 40 ha Kansas USA fields

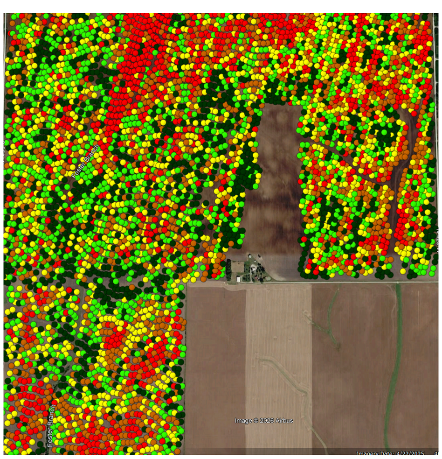

Figure 12. Continuous pH map from 300 ha Indiana USA field

The standard Veris calibration was performed on the example maps in Fig. 9-12 (Lund et al. 2015). Six lab calibration points were selected from each field and soil pH at those points was lab-analyzed. Sensor data with 10 meters of the lab-tested point were paired and a linear regression developed. Each platform showed similar correlation and errors compared to soil lab testing (Table 1).

Table 1. Sensor accuracy metrics for maps shown in Fig. 9-12

		Sensor Accuracy				
pH Type	R^2	*RMSE*	*SD*	*RPD*	*Min*	*Max*
Continuous	0.82	0.20	0.50	2.58	5.4	6.4
Automated Point	0.86	0.20	0.61	3.01	5.85	7.4
Manual	0.88	0.21	0.72	3.43	4.94	6.73

Sampling Density and Modeling pH

Previous research has demonstrated that soil pH sampling densities of approximately 0.2 to 0.4 ha can provide high levels of spatial accuracy; however, such sampling intensities are often economically impractical when relying solely on conventional laboratory analysis (Wollenhaupt and Wolkowski 1994; Mallarino and Wittry 2004). In contrast, field-based pH sensing systems have been demonstrated to measure soil pH at densities ranging from approximately 1 to more than 20 measurements per ha while maintaining acceptable agreement with laboratory methods (Adamchuk et al. 2007).

To quantify the effect of sampling density on pH characterization, eighteen agricultural fields from the Upper Midwest were selected for evaluation. Dense on-the-go pH measurements were used to generate the reference surface and simulated sampling densities ranging from 0.25 to 4 ha. These datasets were used to assess the relationship between sampling density and pH mapping accuracy.

In addition, the same eighteen fields were used to evaluate a remote sensing and terrain-based pH modeling framework similar to that described by Yuzugullu et al. (2024). Sentinel-2 imagery (European Space Agency, n.d.) and terrain attributes derived from high-resolution digital elevation models (U.S. Geological Survey 2024) were used to predict soil pH at a 10-m resolution. The resulting modeled pH surfaces were evaluated independently and in combination with the various sampling density scenarios to determine whether remote sensing could improve pH estimation accuracy and reduce the number of field pH measurements required for practical implementation.

This approach enabled direct comparison of three strategies for spatial pH characterization: (1) sampling alone, (2) remote sensing and terrain modeling alone, and (3) remote sensing and terrain modeling combined with field sampling.

Table 2. Field measurements

Field Stats					
Field ID	*Area (ha)*	*Mean pH*	*Min pH*	*Max pH*	*SD pH*
1	60.6	6.66	4.43	8.32	0.9
2	69.6	6.14	4.95	7.46	0.45
3	55.6	6.46	4.83	7.99	0.53
4	31.3	6.47	4.6	8.27	0.65
5	28.9	6.6	4.64	8.1	0.77
6	21.6	6.52	4.72	7.68	0.53
7	48.6	6.23	4.06	7.65	0.61
8	52.8	6.25	5.14	7.83	0.49
9	18.8	5.84	5.48	6.68	0.23
10	28.1	6.44	5.03	7.74	0.58
11	36.8	5.83	4.6	7.6	0.57
12	31.4	6.71	5.98	7.16	0.19
13	40.6	5.81	4.85	7.22	0.39
14	14.2	6.62	5.05	8.16	0.65
15	31.4	7.24	5.41	8.05	0.5
16	45.7	6.49	5.79	7.47	0.26
17	14.5	6.2	4.44	8.08	0.85
18	37.4	6.31	4.82	8.13	0.53
Overall	667.9	6.38	4.06	8.32	0.54

To produce the dense reference surface and the various sampling-density scenarios used for evaluation, continuous on-the-go soil pH measurements were collected across each field. A 0.1-ha reference surface was selected to serve as the benchmark against which lower sampling densities of 0.25, 0.4, 1, 2, and 4 ha were compared. For each density, sampling locations were selected from the original dense dataset and interpolated using inverse distance weighting (IDW). The reference and all reduced-density datasets were subsequently interpolated to a common 10-m grid, allowing direct cell-by-cell comparison across the entire field (Fig. 13 and Fig. 14).

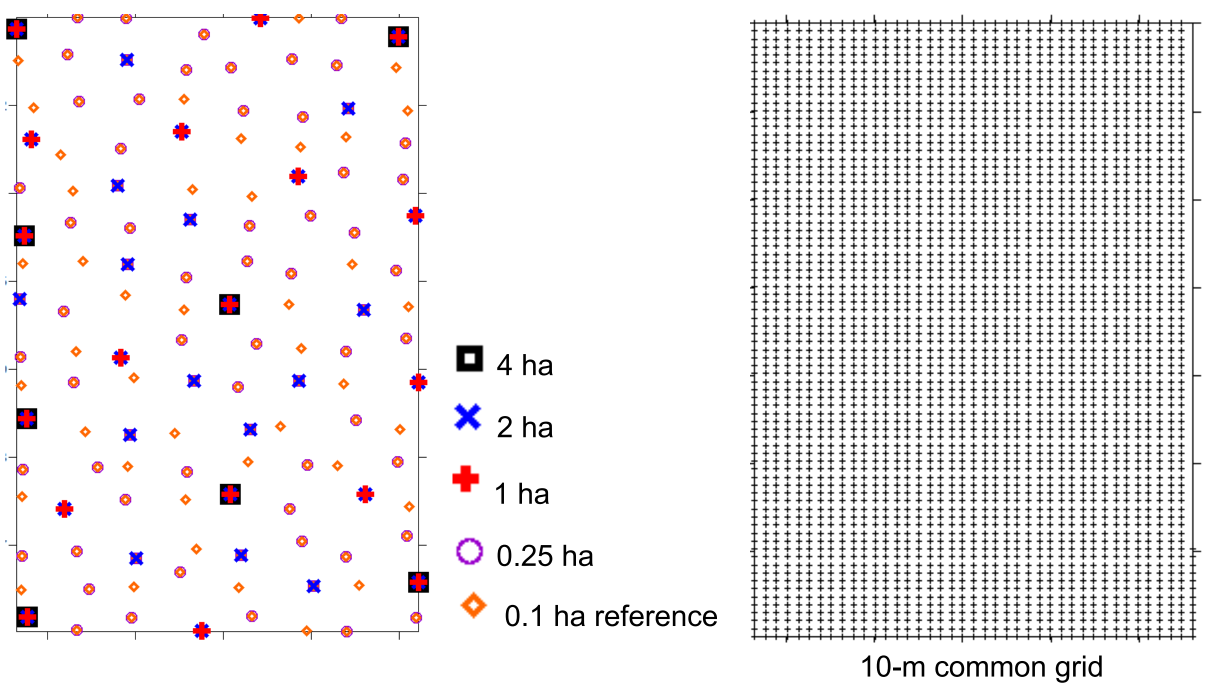

Fig. 13 and Fig. 14 Example of methodology used to convert each sampling density to a common 10 m analysis grid

Results

Map Visualization

The interpolated maps for each sampling density illustrate the diminished detail as sampling density decreases (Fig. 15).

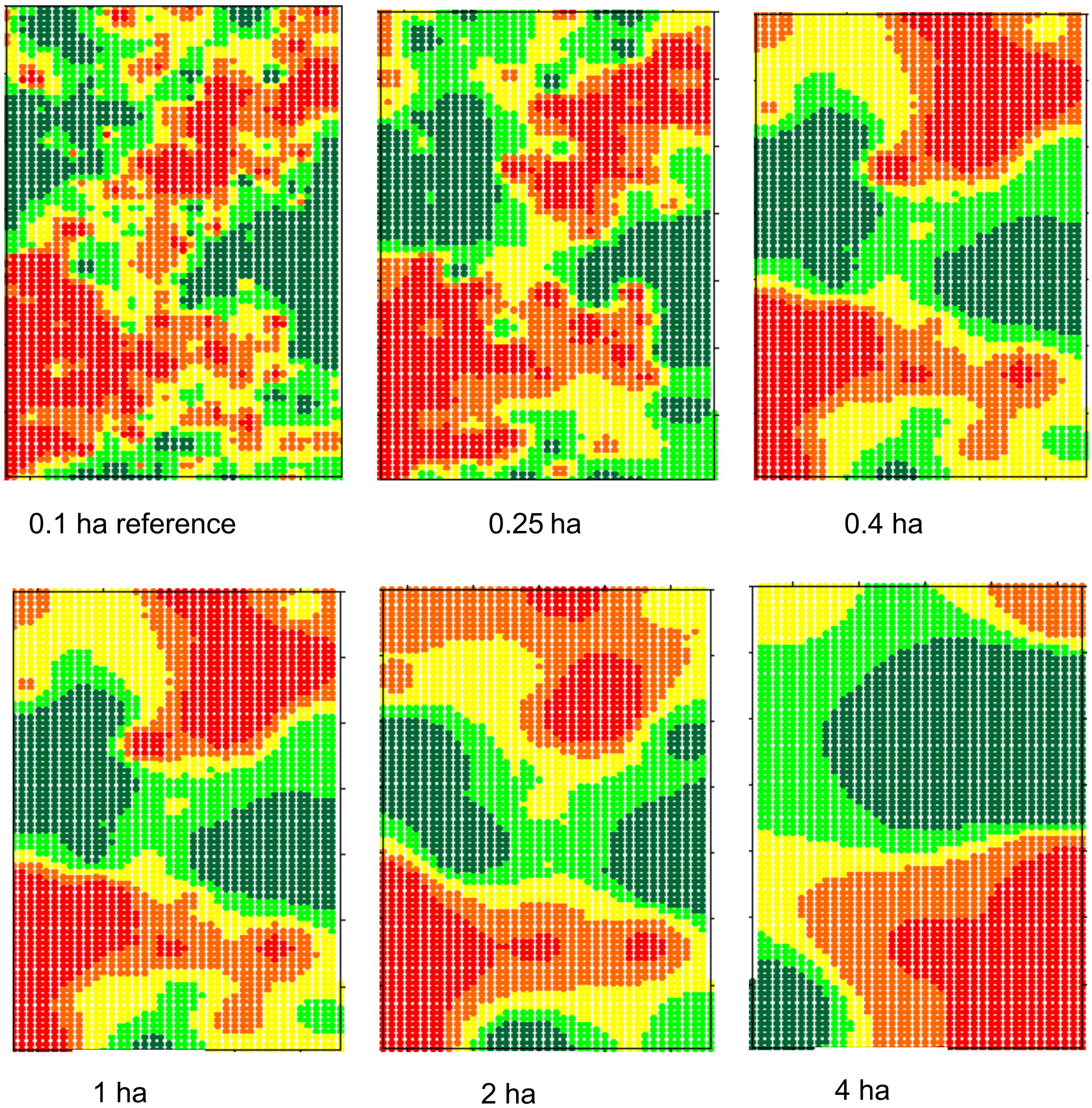

Fig. 15 Map examples of the various sampling densities

Accuracy Results

To develop the machine-learning dataset, the eighteen validation fields were represented by their 10-m reference pH surfaces and paired with remote sensing and terrain variables. Remote sensing predictors were derived from Sentinel-2 surface reflectance imagery (European Space Agency, n.d.) and included spectral bands and bare-soil indices. Terrain predictors were derived from the USGS 3DEP 1-m digital elevation model (U.S. Geological Survey 2024) and included elevation, relative elevation (200-m neighborhood), topographic position index (TPI), topographic wetness index (TWI), and stream power index (SPI). A total of 20 predictor variables were matched to 72,729 observations across the 18 fields and used for model development. Model validation was performed using a leave-one-field-out (LOFO) approach, in which each field was withheld in turn and predicted using a model trained on the remaining 17 fields.

After generating a modeled pH surface for each validation field, the modeled pH was combined with each sampling-density scenario to evaluate whether limited field sampling could improve prediction accuracy. Residual errors between the modeled pH and the sampled grid points were calculated at each available sample location and interpolated across the field using IDW. A final corrected pH estimate was then calculated for every 10-m grid cell as:

Equation 1.

$$pH_{final} = pH_{model} + Residual$$

This residual correction approach preserved the broad spatial patterns captured by the machine-learning model while incorporating local information from field measurements. The procedure was repeated for each sampling density, allowing direct comparison of modeled estimate alone, grid sampling alone, and the combined model estimate and support sampling approach.

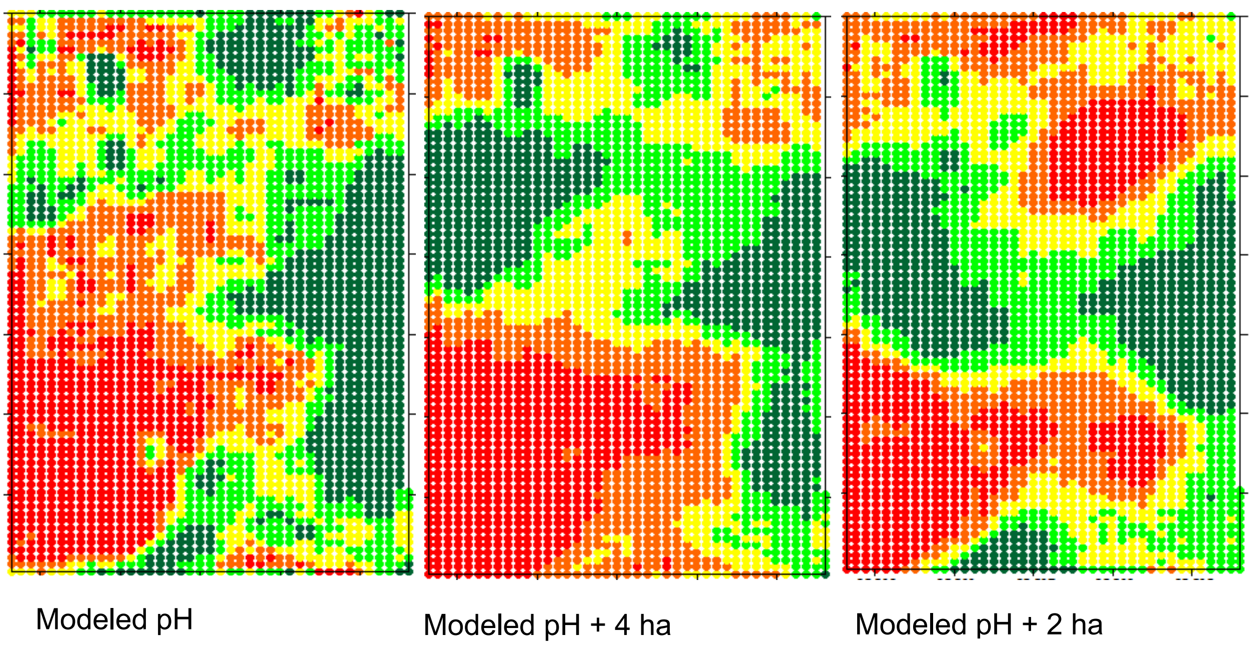

Fig. 16 Example of the leave-one-field-out modeled pH and two iterations of modeled pH supported by grid sampling

A common field average representing conventional composite sampling was used as a baseline for comparing accuracy. The field average pH value was calculated using a simulated W-pattern composite sampling approach. This value was assumed to represent the entire field and was assigned to every 10-m grid cell within the reference surface. The resulting field average prediction was then compared to the 0.1 ha reference pH dataset. Root mean square error (RMSE) was calculated across all grid cells. Grid based and modeled + grid-based interpolation methods were evaluated similarly by comparing interpolated pH values at each 10-m grid cell to the corresponding 0.1 ha reference grid pH value. Improvement relative to the field-average approach was calculated as:

Equation 2.

$$\%\ Improvement = \frac{RMSE_{Field\ Average} - RMSE_{Method}}{RMSE_{Field\ Average}} \times 100$$

RMSE Field Average = RMSE obtained using the W-pattern field-average pH value assigned to the entire field

RMSE Method = RMSE obtained using the evaluated sampling density or modeling approach

Table 3. Results from 18-field study of sampling densities with and without modeling

Grid only (ha)	*RMSE*	*% Improvement vs Field Ave.*	*Model + Grid (ha)*	*RMSE*	*% Improvement vs Field Ave.*
0.25	0.34	35.1%	0.25	0.34	32.7%
0.4	0.36	29.6%	0.4	0.37	28.0%
1	0.45	12.9%	1	0.44	13.5%
2	0.48	4.7%	2	0.47	6.1%
4	0.55	-6.5%	4	0.53	-3.0%
			Model only	0.70	-45.9%

For the grid spacing comparison, the greatest pH mapping accuracy was observed at sampling intensities greater than one sample per hectare. Sampling densities of 1 and 2 ha per sample showed diminished accuracy, while the 4 ha density produced errors greater than those associated with a uniform field-average pH estimate. Similar findings have been reported elsewhere, where increasing sampling density improved pH mapping accuracy, but coarse sampling intervals (>1 ha per sample) provided only limited improvement over field average management (Brouder et al. 2005).

Results and Discussion

Three unique pH deployment methods were evaluated. Each approach demonstrated similar agreement with laboratory pH measurements; however, sampling density and operational requirements differed substantially among systems. These differences allow each method to be deployed in production environments ranging from broad acre row crop agriculture to specialty and smallholder systems.

The simulated sampling density analysis demonstrated the importance of spatial resolution for accurately characterizing within field pH variability. All grid-based approaches except the 4 ha density improved upon the field-average benchmark. The largest incremental gain occurred when sampling density increased from approximately 1 ha to 0.4 ha. These results indicate value in technologies capable of rapidly and economically collecting pH measurements at higher spatial densities.

The modeling approach provided modest improvements compared with interpolation of sample points alone. Benefits were generally small at high sampling densities but increased as sampling density decreased. The greatest improvements were observed when field measurements were incorporated as support samples to correct the modeled pH surface. This finding suggests that modeling pH can complement field sampling, but that some level of field-based measurement is required to achieve acceptable accuracy for management decisions.

Future research will focus on expanding the training dataset and incorporating additional environmental, soil, and remote sensing variables to further improve model performance.

References

Adamchuk, V., E. Lund, T. Reed, and R. Ferguson. 2007. Evaluation of an on-the-go technology for soil pH mapping. Precision Agriculture 8(3):139-149.

ASAE S313.3. Soil cone penetrometer.

Brouder, S.M., B.S. Hofmann, and D.K. Morris. 2005. Mapping soil pH: Accuracy of common soil sampling strategies and estimation techniques. Soil Sci. Soc. Am. J. 69:427-441.

European Space Agency (ESA). n.d. Copernicus Sentinel-2 Level-2A Surface Reflectance Imagery. Accessed via Google Earth Engine. Last accessed 23 June 2026.

Lund, E.D., C.R. Maxton, and T.J. Lund. 2015. Assuring data quality and providing actionable maps using a multi-sensor system. Proceedings of Global Workshop on Proximal Soil Sensing. Hangzhou, China. 266-278.

Mallarino, A.P., and D.J. Wittry. 2004. Efficacy of grid and zone soil sampling approaches for site-specific assessment of phosphorus, potassium, pH, and organic matter. Precision Agriculture 5:131-144.

U.S. Geological Survey. 2024. 3D Elevation Program (3DEP). U.S. Geological Survey, Reston, Virginia, USA. Available at: https://www.usgs.gov/3d-elevation-program. Last accessed 23 June 2026.

Wollenhaupt, N., and R. Wolkowski. 1994. Grid soil sampling. Better Crops.

Yuzugullu, O., N. Fajraoui, and F. Liebisch. 2024. Soil Texture and pH Mapping using Remote Sensing and Support Sampling. IEEE Journal of Selected Topics in Applied Earth Observations and Remote Sensing 17:12685-12705.